

The Structure of Vitellogenin Provides a Molecular Model for the Assembly and Secretion of Atherogenic Lipoproteins

Christopher J. Mann¹, Timothy A. Anderson⁴, Jacqueline Read¹
S. Ann Chester¹, Georgina B. Harrison¹, Silvano Köchl⁵
Penelope J. Ritchie¹, Paul Bradbury¹, Farhana S. Hussain¹
Joanna Amey¹, Berlinda Vanloo⁶, Maryvonne Rosseneu⁶
Recaredo Infante⁷, John M. Hancock², David G. Levitt⁴
Leonard J. Banaszak⁴, James Scott^{1,3*} and Carol C. Shoulders¹

¹MRC Molecular Medicine Group, ²Gene and Genome Evolution Group, Clinical Sciences Centre and ³National Heart and Lung Institute Imperial College School of Medicine, Hammersmith Hospital, London W12 0NN UK

⁴Department of Biochemistry University of Minnesota Medical School, 435 Delaware Street SE, Minneapolis MN 55455-0326, USA

⁵Institut für Gerichtliche Medizin, Müllerstrasse 44 6020 Innsbruck, Austria

⁶Department of Biochemistry Laboratorium voor Lipoproteïne Chemie, University of Gent Hospitaalstraat 13, 8-9000 Gent Belgium

⁷Centre de Recherche INSERM 184 rue du Faubourg St. Antoine, F-75571 Paris Cedex 12, France

The assembly of atherogenic lipoproteins requires the formation in the endoplasmic reticulum of a complex between apolipoprotein (apo)B, a microsomal triglyceride transfer protein (MTP) and protein disulphide isomerase (PDI). Here we show by molecular modelling and mutagenesis that the globular amino-terminal regions of apoB and MTP are closely related in structure to the ancient egg yolk storage protein, vitellogenin (VTG). In the MTP complex, conserved structural motifs that form the reciprocal homodimerization interfaces in VTG are re-utilized by MTP to form a stable heterodimer with PDI, which anchors MTP at the site of apoB translocation, and to associate with apoB and initiate lipid transfer. The structural and functional evolution of the VTGs provides a unifying scheme for the invertebrate origins of the major vertebrate lipid transport system.

© 1999 Academic Press

*Corresponding author

Keywords: vitellogenin; apolipoprotein B; microsomal triglyceride transfer protein

Abbreviations used: apoB, apolipoprotein B; MTP, microsomal triglyceride transfer protein; PDI, protein disulphide isomerase; VTG, vitellogenin; VLDL, very low-density lipoproteins; ER, endoplasmic reticulum; ABL, abetalipoproteinaemia; LDL, low-density lipoprotein; LV, lipovitellin; *M.s.*, *Manduca sexta*; *D.m.*, *Drosophila melanogaster*; ALP, apolipoprotein; RFBP, retinoid fatty acid binding protein; HA, haemagglutinin; *H.s.*, human; *X.l.*, *Xenopus laevis*; *F.h.*, killifish; *I.u.*, lamprey; *B.t.*, bovine; *M.m.*, mouse; *M.a.*, golden hamster; *G.g.*, chicken; *A.t.*, white sturgeon; *O.m.*, rainbow trout; *C.e.*, *Caenorhabditis elegans*; *O.s.*, rhabditid nematode; SD, standard deviation.

E-mail address of the corresponding author: jscott@rpms.ac.uk

Introduction

Chylomicrons and very low-density lipoproteins (VLDL) are among the largest macromolecular complexes (500 to 10,000 Å) secreted from eukaryotic cells. The assembly of neutral lipids and phospholipids into chylomicrons and VLDL is nucleated around a single molecule of apolipoprotein (apo)B in the endoplasmic reticulum (ER). This process has an absolute requirement for a microsomal triglyceride transfer protein (MTP) complexed to an ER-resident chaperone and disulphide bond forming enzyme, protein disulphide isomerase (PDI; Wetterau *et al.*, 1991; Leiper *et al.*, 1994; Gordon *et al.*, 1994). Defects of the apoB and MTP

tein (apo)B in the endoplasmic reticulum (ER). This process has an absolute requirement for a microsomal triglyceride transfer protein (MTP) complexed to an ER-resident chaperone and disulphide bond forming enzyme, protein disulphide isomerase (PDI; Wetterau *et al.*, 1991; Leiper *et al.*, 1994; Gordon *et al.*, 1994). Defects of the apoB and MTP

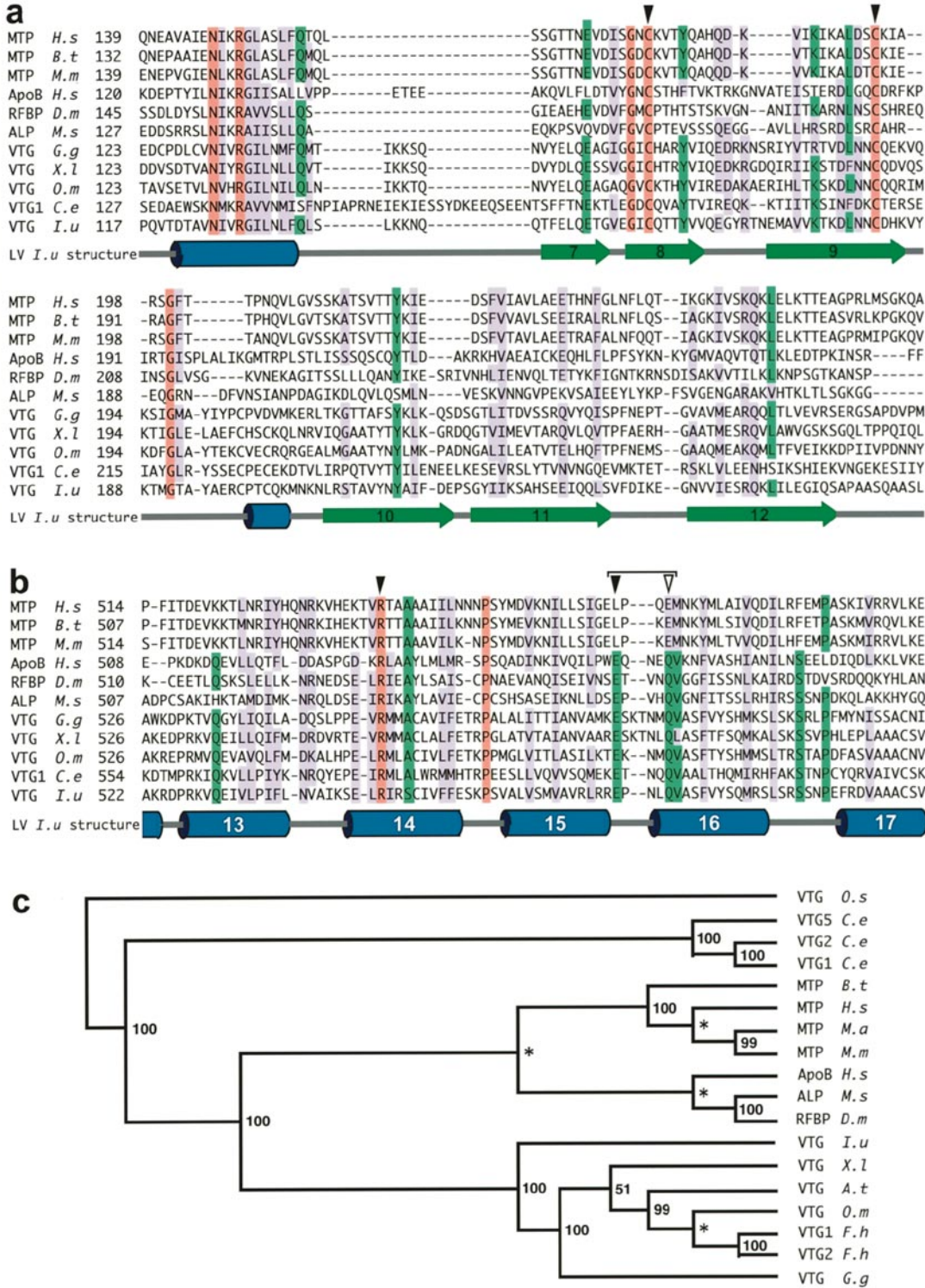


Figure 1. (legend opposite)

genes cause hypobetalipoproteinemia (Linton & Farese, 1997) and abetalipoproteinemia (ABL), respectively (Sharp *et al.*, 1993; Shoulders *et al.*, 1993; Narcisi *et al.*, 1995; Ricci *et al.*, 1995; Rehberg *et al.*, 1996). Affected individuals secrete no normal apoB-containing lipoproteins and have malabsorption of dietary fat and of the fat-soluble vitamins. Deficiency of the antioxidant fat-soluble vitamin E leads to the development of spinocerebellar and retinal degeneration (Kane & Havel, 1989).

ApoB100 is the hepatic form of apoB and is a large (512 kDa, 4563 amino acid residues) monomeric lipid transport protein (Knott *et al.*, 1986; Yang *et al.*, 1986). The amino terminus of apoB100 is rich in disulphide bonds and adopts a compact globular structure (Yang *et al.*, 1990; Segrest *et al.*, 1994; Chatterton *et al.*, 1995). This domain undergoes an independent folding and maturation process, the completion of which may initiate the lipoprotein assembly process (Shelness & Thornburg, 1996). The remainder of apoB forms a belt-like structure wrapped around the surface of the lipoprotein (Chatterton *et al.*, 1995) and contains extensive regions of amphipathic α -helices and β -sheets (Knott *et al.*, 1986; Segrest *et al.*, 1994). The carboxyl-terminal domain of apoB100 also contains the recognition sequence for the receptor-mediated clearance of low density lipoprotein (LDL), the product of VLDL catabolism, from the circulation (Law & Scott, 1990; Welty *et al.*, 1995). LDL is the *agent provocateur* of atherosclerosis.

The amino termini of apoB and of MTP have been proposed to have primary sequence homology with the vitellogenins (VTGs; Baker, 1988; Shoulders *et al.*, 1994). The VTGs are ancient lipid transport and storage proteins that serve as ligands for the delivery of nutrients to the egg yolk by pro-

teins of the LDL-receptor superfamily (Byrne *et al.*, 1989; Bujo *et al.*, 1995; Brown *et al.*, 1997). The crystal structure of lamprey lipovitellin (LV), the mature form of VTG, has been established (Timmins *et al.*, 1992; Raag *et al.*, 1988) and the amino acid residues now assigned (Anderson *et al.*, 1998). LV comprises a globular amino-terminal β -barrel, an extended α -helical structure and a substantial carboxyl-terminal lipid-binding cavity lined by two β -pleated sheets. LV forms a homodimer in which the β -barrel of each subunit interacts with the α -helical domain of the other subunit.

The structures of apoB and of the MTP-PDI heterodimer are unknown and this leaves unresolved a number of important questions relating to the structural relationships between the VTGs, apoB and MTP and the nature of the interactions of apoB with the MTP-PDI heterodimer during the lipoprotein assembly process. Here we have used a modelling approach to address these issues. We have examined the consequences of modelling the amino termini of apoB (amino acid residues 1-587) and of MTP (amino acid residues 22-603) on that of crystalline lamprey LV and examined experimentally the probability that apoB and MTP adopt the predicted structures. The results are affirmative and we conclude that the probabilities of the models being correct are high. In addition, we have mapped the sites of interaction of MTP with both PDI and apoB, and rationalised these in terms of the modelled apoB and MTP structures. The results reveal unexpected structural and functional relationships between the VTGs, apoB and MTP and show how the major structural differences between these proteins relate specifically to their different lipid binding and lipid transfer properties.

Figure 1. Sequence alignment and phylogenetic analysis of the VTG family members. a, Alignment of the amino-terminal homodimerization interface of lamprey LV with other VTGs, MTPs, apoB and of two apoB insect homologues, *Drosophila melanogaster* (*D.m*) retinoid/fatty acid binding protein (RFBP) and tobacco hornworm (*Manduca sexta*; *M.s*) apolipoprotein (ALP). LV is the VTG gene product. The conserved cysteine residues are indicated with arrowheads. Comparison of amino acid residues 1-297 of lamprey (*L.u*) VTG with the corresponding sequences of human (*H.s*) apoB, *D.m* RFBP, *M.s* ALP and *H.s* MTP reveals that the percentage identities and similarities in this domain are: 19.4 and 35.5; 17.1 and 34.2; 17.6 and 39.4; and 20.7 and 41.8, respectively. b, Sequence alignment of helices 13-17 of the α -helical domain of lamprey LV and other members of the VTG gene family. The residues of the buried salt bridge are highlighted with arrowheads. The bracketed arrowheads indicate the use of an alternative glutamate residue in the MTPs. The predicted α -helical domains of *H.s* apoB, *D.m* RFBP, *M.s* ALP and *H.s* MTP have 24.0, 20.1, 21.0 and 18.2 percent identity and 44.3, 38.9, 41.3 and 37.9 percent similarity with amino acid residues 298-607 of *L.u* VTG. c, A phylogenetic tree of the VTG gene family. The numbers are bootstrap percentages and are derived from the consensus tree. Those bootstrap percentages that could not be transferred from the consensus tree are indicated by an asterisk. The major difference between this tree, which represents 18.4% of those obtained, and the consensus tree is that the two insect proteins are placed in the same phylogenetic grouping as apoB. This accords with their similar neutral lipid transport roles and the fact that the insect proteins share primary sequence homology to apoB throughout their entire length (data not shown). The *P*-values for the alignment of amino acid residues 1-3351 of RFBP and 1-3305 of ALP with amino acid residues 1-3475 of apoB are 9.4×10^{-27} and 4.7×10^{-23} , respectively. In a and b, the alignments were generated from 18 sequences; 11 are shown. Residues identical in all 18 sequences are shaded pink. The residues equivalent to R128 and P559 of *L.u* VTG are also shaded pink but are identical in only 17 sequences: R128 is a lysine residue in *O.s* VTG and P559 is a leucine residue in *F.h* VTG2. Residues in green are identical in 13 or more sequences. Residues in mauve have a similarity value > 0.5 (Schwartz & Dayhoff, 1979) in 13 or more sequences. The blue cylinders indicate α -helices. The green arrows depict the six β -strands of the homodimerization interface of *L.u* LV. With the exception of apoB, sequence numbers include the signal peptide.

Results

ApoB and MTP are members of the VTG gene superfamily

To establish whether apoB and MTP might share a common ancestry with the major lipid transport systems of invertebrates, as suggested by previous studies (Baker, 1988; Shoulders *et al.*, 1994; Kutty *et al.*, 1996) we performed a phylogenetic analysis. This was based on an alignment of the first 650 amino acid residues of human apoB, four mammalian MTPs, tobacco hornworm (*Manduca sexta*; *M.s*) apolipoprotein (ALP), *Drosophila melanogaster* (*D.m*) retinoid/fatty acid binding protein (RFBP) and 11 VTGs (Figure 1a and b). The resulting evolutionary tree comprises three major phylogenetic groupings (Figure 1c). The first contains the VTGs of the nematode, the second, the mammalian MTPs, human apoB and the two insect proteins, RFBP and ALP, and the third, the VTGs of the chordates. Thus, both apoB and MTP and the major lipid transport system of arthropods share a common ancestry with the VTGs of the nematodes.

The amino-terminal β -barrel of LV is conserved in MTP and apoB

The finding that both MTP and apoB are members of the VTG gene family raised the question as to whether the tertiary structure of apoB, MTP and VTG in regions of amino acid sequence homology might be similar. To evaluate this we derived and tested, by extensive site-mutagenesis molecular models of MTP (amino acid residues 22-603) and apoB (amino acid residues 1-587) based on the crystal structure of lamprey LV, the mature product of the VTG gene (Figure 2).

The crystal structure of lamprey LV has been refined to an *R*-factor of 19% at 2.8 Å. It reveals that the amino-terminal domain (amino acid residues 17-296) of lamprey LV forms three α -helices and a 13-stranded β -pleated sheet (Anderson *et al.*, 1998); 11 of the strands form a barrel-like conformation. This structure is stabilised by a disulphide linkage (C156-C182) between β -strands 8 and 9. The barrel has a gap between strands 6 and 7, which prevents the formation of a continuous surface by the β -structure. The gap is closed off by a 14-residue α -helix (amino acid residues 121-134), which sits in the shell formed by the β -pleated sheet. The helix contains a highly conserved arginine residue (R128) which extends to the aqueous surface (Figure 1a). The other residues of this helix are less solvent exposed.

Important evidence for the correctness of the MTP and apoB models was provided by the finding that all the cysteine residues in apoB and MTP formed appropriate disulphide linkages (Figure 2a-d). In addition, both models had good geometry and chemical contacts. With the exception of glycine residues, and K256 and L494 of apoB, and D30, N31 and E342 of MTP, all residues

were in the allowed region of a Ramachandran plot and had normal non-covalent interactions (data not shown). In the models, K256 and L494 of apoB and D30, N31 and E342 of MTP are predicted to reside in loop structures.

The models of the amino-terminal regions of MTP (amino acid residues 22-603) and apoB (amino acid residues 1-587) predict conservation of the barrel-like structure of LV and of the central helix with its highly conserved arginine residue in both MTP and apoB (Figures 1a, 2a and 2b). As in LV, and predicted for MTP and apoB, the two cysteine residues homologous to lamprey LV C159 and C185 tie together strands 8 and 9 of the amino-terminal β -sheet. Mutation of either or both of these residues in MTP and apoB is deleterious (Figure 3(a) and (b)). These results indicate that the β -barrel of lamprey LV is conserved in MTP and apoB.

The α -helical domain of LV is conserved in MTP and apoB

The α -helical domain (amino acid residues 297-614) of lamprey LV comprises 17 α -helices arranged in a double-layered, super-helical configuration (Raag *et al.*, 1988). The inner helices reside towards the centre of the molecule and form a series of stabilising intramolecular contacts. The inner helices 6, 8 and 10 form the apex of the lipid-binding cavity. The central portion of the domain is stabilised by a disulphide linkage (C451-C486). The surface of the outer helices 13, 15 and 17 are used in homodimerization. This part of the structure contains a completely buried salt bridge formed between R547 and E574. This ties together helices 14 and 16, thereby increasing the stability of the local fold. R547 resides at the fourth position of helix 14 where it makes two hydrogen bonds with E574. The estimated bond lengths are 3.01 Å and 2.93 Å. The pairing involves the first and second nitrogen atoms of R547, but not the N^εH atom, which interacts with the main-chain carbonyl group oxygen atom of F537 and N539.

The predicted α -helical domains of MTP (amino acid residues 304-598) and apoB (amino acid residues 294-592) comprise 17 helices arranged in an inner and outer layer. As in LV, the central portions of the helical structures are stabilised by a disulphide linkage. The buried salt bridge of LV is also predicted. To evaluate the models of the α -helical domains of MTP and apoB we examined the importance of the LV conserved buried salt bridge. In MTP, the amino acid residue homologous to lamprey LV R547, MTP R540, is placed at the third position of helix 14, completely buried within the α -helical structure, whereas all other arginine and lysine residues occupy more exposed positions. The model identifies two residues, N531 and E570, that might hydrogen bond with R540 to form a fully buried salt bridge, thereby satisfying all of the protons of R540 (Figure 2e). N531 is predicted to be the penultimate residue of helix 13

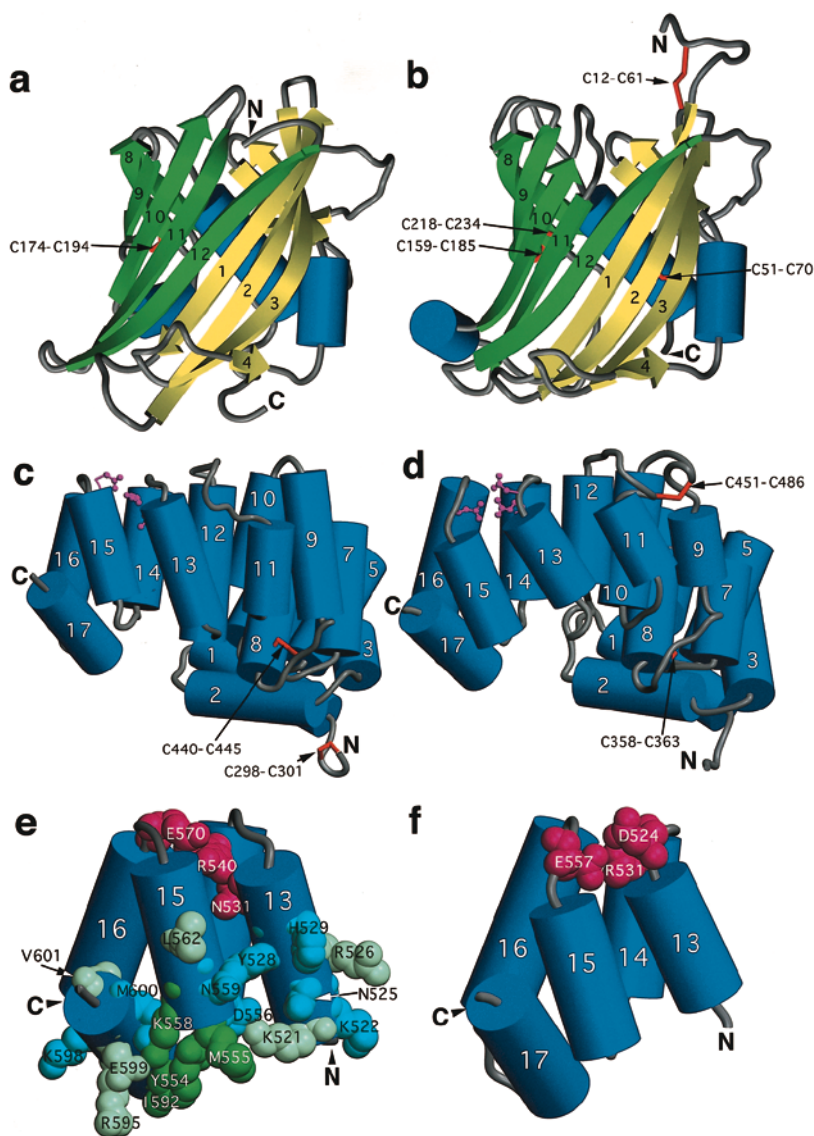


Figure 2. Molecular models of MTP and apoB based on the atomic coordinates of lamprey LV. a, The amino-terminal β -sheet of MTP. Of the 13 β -strands, 11 are arranged in a barrel-like conformation. The strands comprise K34-R46, G56-G74, L79-R96, S106-S108, P122-I128, K131-S137, G163-D169, G172-H181, K184-A190, G209-Y220, S225-G239, I246-A263 and A275-V280. The central helix is formed by residues V143-F156. The two smaller helices comprise K113-Q120 and T202-Q206. β -Strands 7-12 correspond to the homodimerization interface of lamprey LV and are depicted in green. The conserved C174-C194 cystine tethers β -strands 8 and 9. b, The amino-terminal β -barrel of apoB. The β -strands comprise H21-G36, S43-P58, S62-Y76, A84-K88, E104-I109, G112-L117, K147-T154, G157-R168, A173-R187, L211-L222, E231-L241 and N247-D263. The central helix is formed by residues T124-L137. The two smaller helices comprise E93-R101 and G203-L208. The strands of the barrel are stabilized by three cystine groups C51-C70, C159-C185 and C218-C234. The C51-C70 and C218-C234 linkages stabilize four long strands. The C159-C185 cystine links the shorter strands 8 and 9. c, The predicted α -helical domain of MTP. Helices 1-17 comprise L304-N319, A325-T338, E343-L348, L356-V363, T368-F381, S386-G398, E406-S418, I424-C440, V450-K463, K467-K478, P483-L490, L503-I516, V520-R532, T538-N549, D556-E566, M571-I582 and I592-K598, and are arranged in inner

(even numbered) and outer (odd numbered) layers. Helices 8 and 9 are restrained by cystine C440-C445. Side-chain atoms of the buried salt bridge residues R540, E570 and N531 are displayed in magenta. d, The α -helical domain of apoB. Helices 1 to 17 comprise amino acid residues Q294-K307, R317-R329, S332-I344, P349-L355, T365-A376, D382-V388, R400-D408, L415-Y425, D438-M444, D456-E473, T476-I483, M495-L504, Q514-L522, G528-L538, Q544-I553, E560-I573 and Q582-L592. The cystine groups C358-C363 and C451-C486 stabilize helices 4 and 5, and 9 and 10, respectively. e, Expanded view of helices 13-17 of MTP showing the predicted buried salt bridge and PDI-binding residues. Side-chains are depicted as van der Waals spheres. The main-chain and side-chain atoms of R540 and N531 are completely buried, as is the carboxylate group of E570. The NH1 atom of R540 is within acceptable hydrogen-bonding distance of the main-chain carbonyl oxygen atom of N531 and the OD1 atom of N531. The N ϵ and NH2 atoms of R540 are within bonding distance of the OE1 and OE2 atoms of E570, respectively. The OE2 atom of E570 is also within acceptable bonding distance of the ND1 atom of H535. The mutant R540K has near wild-type activity. A lysine residue at position 540 is predicted to form three hydrogen bonds, two with E570 and one with N531. Estimated bond lengths between the NZ atom of K540 and OE1 and OE2 of E570 and OD1 of N531 are 2.7 Å, 2.8 Å and 3.2 Å, respectively. Y554, M555, K558 and I592 participate in PDI binding and are depicted in dark green. K521, R526, N551 (not visible), R595, E599 and V601 make no significant contribution to PDI binding and are shown in pale green. K522, N525, Y528, H529, D556, N559, K598 and M600 are predicted to be predominantly surface-exposed and are shown in pale blue. In lamprey LV, the homologous amino acid residues form part of the α -helical homodimerization interface. Their contribution to MTP-PDI dimerization has not been examined here. f, Expanded view of the R531-E557-D524 buried salt bridge of apoB. NH1 of R531 is predicted to be within hydrogen-bonding distance of the OE2 atom of E557 and the OD1 atom of D524. The NH2 atom is within hydrogen-bonding distance of OE1 and OE2 of E557, the estimated bond lengths being 3.0 Å and 3.2 Å, respectively. The N ϵ H atom of R531 interacts with the main-chain carbonyl oxygen atom of F521. In a to f, α -helices are depicted as blue cylinders, disulphide groups are red, loops are grey and β -strands are yellow, except those that correspond to the homodimerization interface of lamprey LV, which are shown in green.

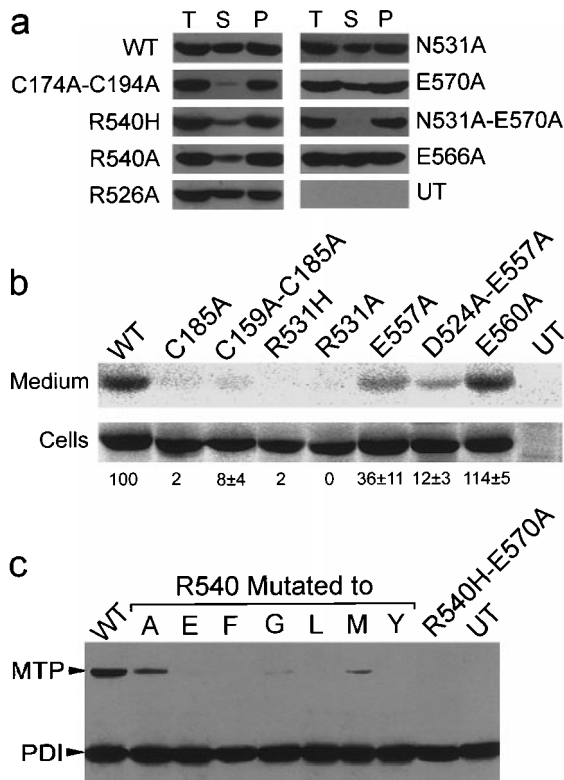


Figure 3. Evaluation of the molecular models of MTP and apoB. (a), Mutation of the MTP C174-C194 disulphide linkage and putative R540-E570-N531 buried salt-bridge residues. Equal aliquots of total (T) Cos-1 cell lysates, soluble (S) and the 100,000 g pellet containing membrane-associated or insoluble proteins (P) were analyzed by SDS-PAGE and immunoblotting. (b), Mutation of the apoB C159-C185 disulphide linkage and putative R531-D524-E557 buried salt-bridge residues. Secretion of mutant forms of apoB17 were studied in Cos-1 cells. The values are the percent of apoB secreted following a two hour chase divided by total intracellular apoB at time zero after a one hour labelling period. Values are the mean \pm standard deviation (SD). Experiments undertaken only twice have no SDs. (c), Western blot analysis of the ability of amino acid residues with varying packing and helix-forming potentials to replace MTP R540. R540 was replaced with residues with high packing and helix-forming potential (M, L, F); high packing and low helix-forming potential (Y), low packing and low helix-forming potential (G) and low packing and high helix-forming potential (A). Soluble fractions are shown. For both (a) and (c), there was good agreement with the triglyceride transfer assays (see Table 1) and the immunoblotting results obtained. UT is untransfected, WT is wild-type MTP.

and to form two hydrogen bonds with R540. E570 is predicted to be the last residue of the loop preceding helix 16 and to make three hydrogen bonds, two with R540 and one with H535. In the apoB model, the amino acid residue homologous to LV R547 and MTP R540, apoB R531 (Figure 2f), resides at the fourth position of predicted helix 14, where it makes three hydrogen bonds with E557,

the fourth residue of the loop connecting helix 15 and 16, and one hydrogen bond with D524, the second residue of the loop connecting helices 13 and 14. The pairing involves the first and second nitrogen atoms of R531, but not the N^εH atom, which interacts with the main-chain carbonyl oxygen atom of F521.

To evaluate the MTP buried salt bridge, N531 and E570 were replaced, separately and together, with alanine. R540 was mutated to alanine and histidine, since the R540H missense mutation causes ABL (Rehberg *et al.*, 1996; C.S. & R.I., unpublished results). E566A and E599A were generated as controls because these residues are predicted to be beyond normal hydrogen-bonding distance of R540. K521, R526, R532, K533, K558, R584, K591, R594, R595 and K598 were also mutated to alanine. These residues, by virtue of their predicted predominantly surface-exposed positions on the MTP monomer, were anticipated to make minimal contribution to the stability of MTP.

The wild-type and mutant MTPs were individually expressed in Cos-1 cells. The amount of soluble MTP and triglyceride-transfer activity were substantially reduced in cells expressing R540H and R540A (Figure 3(a) and Table 1, respectively), despite comparable levels of MTP mass. The amount of triglyceride-transfer activity in cells expressing the single mutants N531A and E570A and the double mutant N531A-E570A was decreased by around 20%, 60% and 95%, respectively (Table 1). The reductions in triglyceride-transfer activities were proportional to the amount of soluble MTP recovered (Figure 3(a)), indicating that the mutation of R540, N531 and E570 affected the production or stability of soluble MTP, rather than directly interfering with its lipid-transfer activity. E566A and E599A, and the mutated residues predicted to occupy surface-exposed positions, had no effect on the solubility (Figure 3(a)) or activity of MTP (Table 1).

Additional explanations for the effect of the mutation of R540 on MTP were considered. First, arginine has a higher helix-forming potential than histidine (O'Neill & DeGrado, 1990). Second, arginine has a greater packing potential than alanine or histidine. To test these possibilities, we replaced R540 with residues of varying sizes and helix-forming potentials. All showed the same dramatic effect on MTP solubility (Figure 3(c)) and activity (Table 1). Third, we considered that the mutant R540 proteins might be destabilised by the unpaired charge of E570 (Tissot *et al.*, 1996). R540 was replaced with lysine and the unpaired charge of E570 in R540H, R540A and R540L removed by alanine substitution. R540K had wild-type activity (Table 1), as described (Rehberg *et al.*, 1996). The other mutants were completely inactive (Table 1).

To evaluate the structural importance of the apoB buried salt bridge (R531-E557-D524), R531A, R531H and E557A were individually created in apoB17. E557A was also mutated with D524A.

Table 1. Summary of mutants

Mutation MTP	LV	ApoB	LV position	MTP activity (% of wild-type)	PDI binding (% of wild-type)
C174A ⁱ	C156	C159	β8,3 ^a	<5	-
C174A-C194A	C182	C185	β10, 12 ^a	<5	-
V520A	V529	D513	h13,3	76	-
K521A	Q530	Q514	h13,4 ^b	70	102
K521A-Y554A-M555A	-	-	-	<5	27
R526A	P535	Q519	h13,9 ^{b,c}	92	101
R526A-Y554A-M555A	-	-	-	7	40
N531A	N539	D523	1p13-14,1 ^d	83	-
R532A-K533A	V540	D524	1p13-14,2	120	-
R532A-K533A	A541	A525	1p13-14,3	120	-
R540H ^{h,k}	R547	R531	h14,3 ^{d,e,f}	<5	86
R540A ⁱ	-	-	-	21	43
N551A-Y554A-M555A	K558	S541	1p14-15,2	49	-
Y554A	V561	Q544	1p14-15,5 ^{c,g}	91	-
Y554A-M555A	-	-	-	53	34
M555A	A562	A545	h15,1 ^{c,g}	94	-
K558A	S565	N548	h15,4 ^{c,g}	73	20
Y554A-M555A-K558A	-	-	-	34	18
L562A	V569	Q552	h15,8 ^c	45	300 ^h
E566A	R573	W556	h15,12 ^c	130	-
L567 ^j	E574	E557	1p15-16,1 ^{e,f}	N/A	N/A
Q569 ^j	L577	E560	h16,1	N/A	N/A
E570A	Q578	Q561	h16,2 ^d	36	-
N531A-E570A	-	-	-	<5	-
R584A-F585A	R592	N575	1p16-17,3	88	-
R584A-F585A	S593	S576	1p16-17,4	88	-
K591A	R599	Q582	h17,1	86	-
I592A	D600	D583	h17,2 ^{c,g}	91	49
Y554A-M555A-I592A	-	-	-	22	14
R594A	A602	K585	h17,4 ^c	107	-
R594A-R595A	-	-	-	94	-
R595A	A603	K586	h17,5	139	-
K598A	S606	K589	h17,8 ^c	83	-
E599A	V607	E590	h17,9 ^c	117	82
Y554A-M555A-E599A	-	-	-	12	46
V601A	I609	I592	1p17,2	87	-

For LV position, β, h and 1p denote β-strands of the amino-terminal barrel, and helices and loops of the α-helical domain of lamprey LV (followed by residue number), respectively.

^a Highly conserved cysteine residues;

^b Predicted neighbour to Y554 or M555;

^c Dimerization residue in lamprey LV homodimer;

^d Salt bridge residue in MTP

^e Salt bridge residue in LV;

^f Salt bridge residue in apoB;

^g PDI binding residue in MTP;

^h See Clackson & Wells (1995); Waldburger *et al.* (1995); Nichols & Matthews (1997).

ⁱ Mutated in MTP and apoB.

^j Mutated in apoB only. Triglyceride transfer activity assays were performed as described (Narcisi *et al.*, 1995). Values represent the average of two or more experimental observations.

^k Triglyceride transfer activities of R540E, R540G, R540L, R540T, R540Y, R540A-E570A, R540H-E570A, R540L-E570A and R540T-E570A were less than 5% of wild-type. The corresponding values for R540M and R540K were 15% and 93% of wild-type, respectively.

E560A was created as a control for E557A as it is predicted to occupy a predominantly solvent-exposed position. The mutation of R531A, R531H and double mutant E557A-D524A virtually abolished the secretion of apoB17 from Cos-1 cells, while the secretion of mutant E557A was reduced to 36(±11)% of wild-type. The control mutation had no functional impact (Figure 3(b)). Thus, the effect of mutating E557 and D524, the predicted anionic partners of R531, is consistent with their role in buried salt bridge formation, and is similar in magnitude to mutating the homologous amino acid residues N531 and E570, in MTP (Figure 3(a) and (b); Table 1).

The α-helical domain of MTP binds PDI

MTP forms a stable interaction with PDI and by this is rendered fully soluble and active (Wetterau *et al.*, 1991; Lamberg *et al.*, 1996). Initial attempts to map the site of interaction of MTP with PDI were confounded by the insolubility of GST/MTP fusion proteins (unpublished results) and of carboxyl-terminally truncated forms of MTP (Narcisi *et al.*, 1995; Ricci *et al.*, 1995). We therefore studied the MTP-PDI interaction using a yeast two-hybrid system. The MTP constructs encoded the amino-terminal β-barrel sheet, the α-helical region and the carboxyl-terminal domain (Figure 4a). Each was

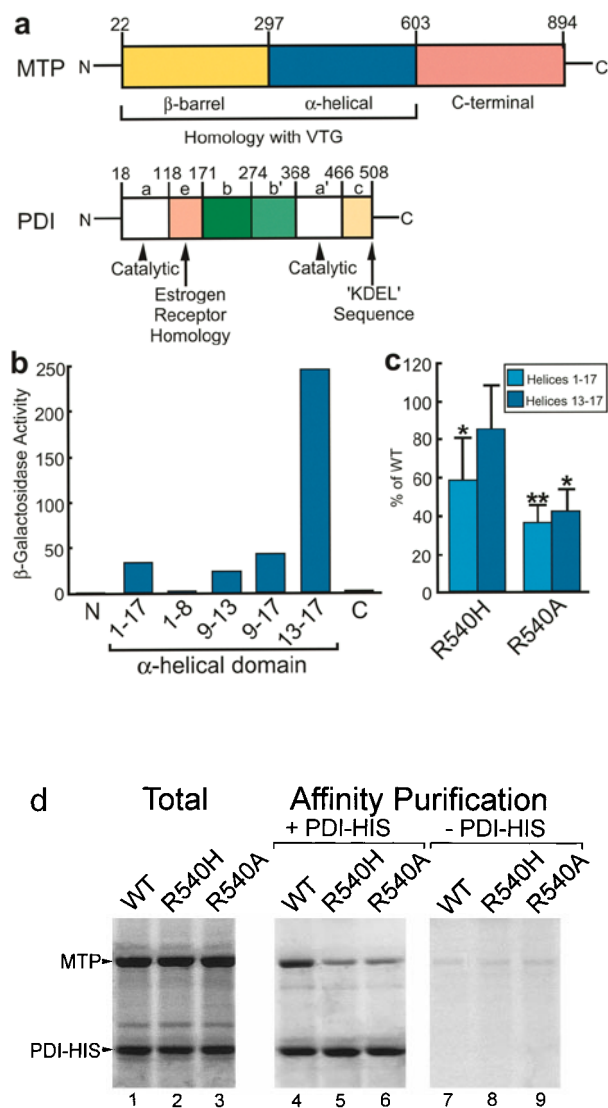


Figure 4. The α -helical domain of MTP binds PDI. **a**, Proposed domain organizations of MTP and PDI. The **b** and **b'** domains of PDI share sequence similarity to each other but not to any other protein. **b**, Helices 13-17 of the predicted α -helical domain of MTP interact with PDI-aeb in the yeast two-hybrid system. β -Galactosidase activity was assayed as described (Reynolds & Lundblad, 1992). The results are the mean of five observations, minus the value of the control bait plasmid. N and C represent the predicted amino-terminal β -barrel and carboxyl-terminal lipid-binding domains, respectively. **c**, Interaction of R540 mutants with PDI. R540H and R540A significantly reduced the interaction of the entire α -helical domain of MTP with PDI-aeb ($*P < 0.05$ and $**P < 0.001$ compared to wild-type (WT)). R540A in helices 13-17 also decreased the MTP-PDI interaction. R540H in helices 13-17 had a smaller effect which was not significant. Values are mean \pm SD. **d**, Mutation of R540 impairs the interaction of MTP with PDI in Sf9 cells. Lanes 1-3 show total microsomal contents from Sf9 cells expressing wild-type MTP, MTP R540H and R540A with PDI-HIS. The total level of expression of the mutant MTPs was comparable to the wild-type. Lanes 4-6, show wild-type and mutant MTPs purified with PDI-HIS. Lanes 7-9 show controls for the HIS-purification. The results show one of three similar experiments.

expressed with full-length PDI and with two carboxyl-terminally truncated forms of PDI. These were based on the proposed domain organisation of PDI (Figure 4a).

The predicted α -helical domain of MTP produced the only significant interaction with PDI (Figure 4b). The interaction was around 30-fold higher than with the predicted amino-terminal and carboxyl-terminal domains of MTP. The strongest interaction of PDI with the α -helical domain of MTP was with the PDI construct representing domains a, e and b (Figure 4b). No interaction was observed with PDI-ae. The interaction of PDI-aeb with MTP was confirmed in the baculovirus system (data not shown). The interaction rendered MTP soluble, but not active. MTP was only active when expressed with full-length PDI. Analogous results have been described for prolyl-4-hydroxylase, which forms an α - β tetramer with PDI (Veijola *et al.*, 1996). To fine-map the PDI-binding region on MTP, predicted helices 1-8, 9-13, 9-17 and 13-17 of the α -helical domain of MTP were expressed with PDI-aeb. The data suggest that predicted helices 13-17 of MTP form a major binding site for PDI (Figure 4b). The finding that the binding of PDI to MTP helices 13-17 was around six and fourfold higher than to MTP helices 1-17 and 9-17, respectively, is consistent with the results of previous yeast two-hybrid studies which have shown that other proteins produce higher levels of interaction with their partners when expressed as small sub-domains (Golemis & Brent, 1992; Poortinga *et al.*, 1998). Removal of certain structural motifs from LexA-Myc and LexA-Fos fusion proteins resulted in a five to tenfold increase in their interacting abilities (Golemis & Brent, 1992).

In view of the localisation of the PDI-binding site on the MTP monomer, we considered whether disruption of the buried salt bridge between R540-E570-N531 might impair MTP-PDI dimerization. Previously, it was speculated that R540 might form a salt bridge with a distal site on MTP or with PDI (Rehberg *et al.*, 1996). The MTP-PDI interaction was examined in the yeast two-hybrid system and in the baculovirus system. In the yeast two-hybrid system, the mutations R540H and R540A in the entire α -helical domain of MTP reduced MTP-PDI dimerization to 59(\pm 22)% and 38(\pm 9)% of wild-type, respectively. In helices 13-17, R540H and R540A reduced the interaction to 86(\pm 26)% and 43(\pm 11)% of wild-type ($P < 0.02$ for the difference between R540H and R540A; Figure 4c). In the baculovirus system, the amount of R540H and R540A complexed to PDI was reduced to 14(\pm 1)% and 23(\pm 6)% of wild-type, respectively ($P < 0.05$ for the difference between R540A and R540H; Figure 4d). Thus the loss of the buried R540-N531-E570 salt bridge near the carboxyl terminus of the α -helical domain of MTP perturbs the binding of PDI to the surface of this helical region.

In the LV homodimer, the region homologous to the MTP-PDI interaction site forms five α -helices, 13 to 17, arranged in two layers (Anderson *et al.*,

1998). The inner surface of the inner helices makes extensive intramolecular contacts with the nearby, seven-stranded, β -pleated sheet (amino acid residues 615-688 and 729-758). This sheet forms part of the lipid-binding cavity. The outer convex surface forms extensive subunit contacts with β -strands 7-12 of the amino-terminal β -barrel. The interfacial residues form a hydrophobic plate that encompasses the entire exposed surface of outer helices 13, 15 and 17.

In the model of MTP, overall conservation of the double-layered helical structure of LV is predicted (Figure 2c). The critical R540-E570-N531 salt bridge unites three segments of secondary structure, namely helices 13 and 14 and the loop preceding helix 16 (Figure 2e). T541, A542, A545 and N549 of helix 14 and K573, Y574, A577, I578 and D581 of helix 16 contribute to the inner surface of the inner helices. Residues F585, M587, A589 and S590 in the loop between 16 and 17 are predicted to form a small hydrophobic patch ($\sim 240 \text{ \AA}^2$) at the edge of the helical domain. The larger external surface of the outer helical layer contains around 20 side-chains. A high proportion of these are hydrophobic or charge-neutralised, a feature characteristic of subunit interfaces in other proteins (Sattler *et al.*, 1997; Wang *et al.*, 1994; Janin *et al.*, 1988; Clackson & Wells, 1995). Overall, the aliphatic portions of the residues at the predicted MTP surface occupy an area of around 1900 \AA^2 .

To evaluate the hydrophobic surface of helices 13, 15 and 17 of MTP as the PDI binding site, surface-exposed residues were replaced with alanine and assayed in Cos-1 cells (Table 1). Only the double mutant Y554A-M555A showed reduced solubility (Figure 5a) and activity (Table 1). This mutant protein was analyzed for PDI binding in the yeast two-hybrid system. In the entire α -helical domain of MTP, Y554A-M555A reduced MTP-PDI dimerization to $46.3(\pm 10)\%$ of wild-type. In predicted helices 13-17, the corresponding value was $34.0(\pm 3)\%$. To substantiate the evidence that Y554 and M555 form part of the PDI-binding site on MTP, we created triple mutants based on Y554A-M555A. Predicted neighbours K521, R526 and K558, which are around 6 \AA , 7.5 \AA and 16 \AA from M555, and I592 and E599, which are closer to Y554, were mutated to alanine. Residues N551, R595 and V601, predicted not to contribute to the PDI-binding site, were also mutated. N551 resides at the bottom of a crevice, while R595 and V601 line the exposed face of the carboxyl-terminal end of the α -helical domain of MTP, some distance from Y554 and M555. Mutation of residues predicted to be near to Y554 and M555 virtually abolished the solubility of full-length MTP, when combined with Y554A-M555A. Mutation of other residues had no effect (Table 1; Figure 5a).

To investigate further the role of K521, R526, K558, I592 and E599 in the interaction of helices 13-17 with PDI, we once again used the yeast two-hybrid system (Figure 5b). Single mutants K558A and I592A impaired interaction. E599A had a small-

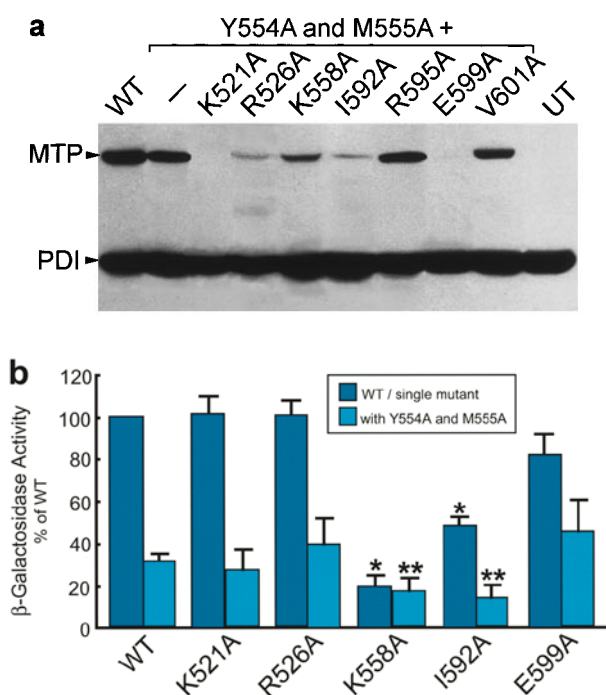


Figure 5. Mutation of the PDI-binding site on MTP. a, Mutation of residues at the surface of helices 13, 15 and 17. Mutant proteins were expressed in Cos-1 cells and analyzed by Western blotting as in Figure 3. Similar results were obtained for each mutant protein in a minimum of three experiments. b, Mutations were introduced into helices 13-17 of MTP and expressed with PDI-aeb in the yeast two-hybrid system. Values are mean \pm SD ($n \geq 10$). The single asterisks indicate significant differences ($P < 0.01$) from wild-type, and the double asterisks the differences from Y554A-M555A.

er effect. K521A and R526A had no effect. Triple mutants Y554A-M555A with K558A or I592A reduced the interaction to below 20% of wild-type. The combination of K521A, R526A or E599A with Y554A-M555A had no additional effect on the binding of MTP to PDI suggesting that they do not form part of the PDI-binding site and that the results observed in Cos-1 cells with these mutants is caused by global destabilisation of full-length MTP. We conclude that Y554, M555, K558 and I592 form part of the major PDI-binding site on MTP, and that the α -helical homodimerization interface in lamprey LV is conserved in MTP and re-utilised as a binding site for PDI.

The β -barrels of apoB and MTP interact

The interaction between the amino terminus of apoB (apoB17) and MTP was investigated by co-immunoprecipitation studies using the baculovirus expression system (Figure 6(a)). To identify the MTP-binding site(s) on apoB17, we evaluated the ability of shorter truncated forms of apoB (apoB3.4, residues 1-152; apoB4.5, residues 1-204; apoB5.8, residues 1-264; apoB11, residues 1-499; apoB13,

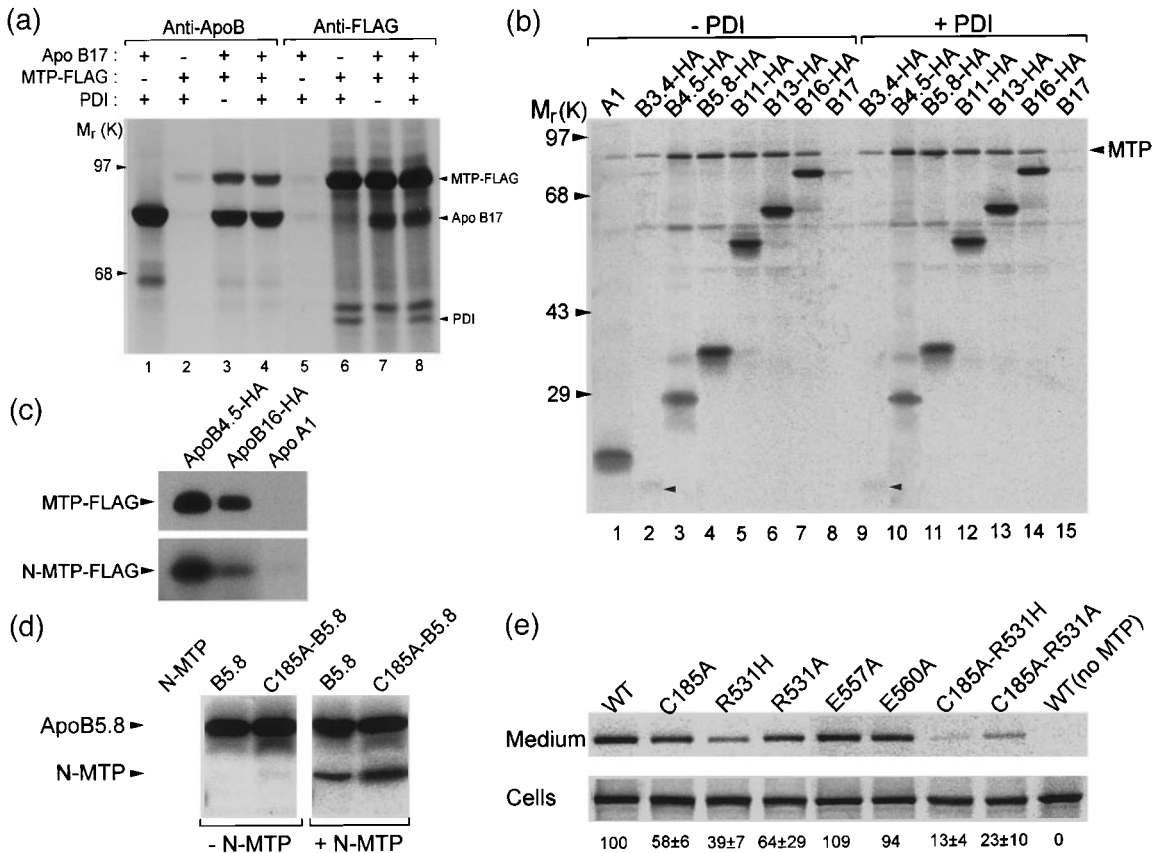


Figure 6. Identification of sites of interaction between apoB and MTP. (a), The interaction of apoB17 with MTP. MTP-FLAG, apoB17 and PDI were expressed in Sf9 cells and labelled with L-[³⁵S]-methionine under steady-state conditions. Immunoprecipitations were performed in 1% (v/v) Triton X-100 (Wu *et al.*, 1996; Gretch *et al.*, 1996; Reynolds & Lundblad, 1992; Patel & Grundy, 1996) to solubilize the lipoprotein assembly complex. Immunoprecipitations were with anti-apoB (lanes 1-4) or anti-FLAG (lanes 5-8). Lane 1 shows that apoB does not bind to PDI. Lanes 3 and 7 show that detergent-solubilized apoB and MTP-FLAG associate in the absence of PDI. Lane 5 is a control for the anti-FLAG antibody. Lanes 6-8 show the association of MTP with PDI and apoB. The amounts of the interacting proteins were determined by phosphorimaging and corrected according to their methionine content. The associations were not stoichiometric. This is probably due to the solubilization of MTP by detergent in the absence of PDI expression. The identities of the 65 kDa protein in lane 1 and of the protein with a similar M_r to PDI in lanes 6 and 8 are not known. (b), The β -barrel of apoB interacts with MTP. Carboxyl-terminally truncated forms of HA-tagged apoB, full-length apoAI and MTP were expressed in Sf9 cells in the absence and presence of PDI. ApoB3.4, 4.5, 5.8, 11, 13 and 16 encode residues 1-152, 1-204, 1-264, 1-499, 1-590 and 1-720 of apoB, respectively. Immunoprecipitations (with anti-HA or anti-apoAI antibodies) were as for (a), and the amounts of the interacting proteins were determined by phosphorimaging and corrected according to their methionine content. Lane 1 shows that the immunoprecipitation of apoAI brought down a small amount of MTP. Lanes 2-6, the arrow in lane 2 indicates that the intracellular level of apoB3.4 is very low. On a mole to mole basis apoB3.4 was associated with the same amount of MTP as apoB4.5-apoB13 (lanes 3-6), and 15-fold more than the control apoAI protein (lane 1). Lane 7 shows that apoB16 is associated with 40% less MTP than apoB3.4-apoB13. Lane 8 is a control for the specificity of the HA antibody. Lanes 9-15 show that the interactions between the apoBs and MTP were unchanged by PDI expression. (c) Western blot analysis of the interaction between the amino termini of MTP and apoB. ApoB4.5-HA, apoB16-HA and apoAI were expressed in Sf9 cells with either MTP-FLAG (top panel) or the FLAG-tagged soluble amino-terminal β -barrel (amino acid residues 1-297) of MTP (bottom panel). Immunoprecipitations were with anti-HA and anti-apoAI. Co-immunoprecipitated MTP-FLAG was detected by immunoblotting. The amino-terminal β -barrel of MTP interacted with apoB4.5. As in (b), apoB16 showed a lower level of interaction with MTP than apoB4.5. (d), Mutation of the apoB C159-C185 disulphide group increases the interaction of the β -barrel of apoB with MTP. ApoB5.8-HA, full-length apoAI and the predicted β -barrel of MTP were expressed in Sf9 cells. Immunoprecipitations were with anti-HA antibodies. The first three lanes show that the mutant apoB5.8 protein immunoprecipitated threefold more MTP than wild-type apoB5.8. (e), Evaluation of the role of the conserved C159-C185 and R531-D524-E557 buried salt bridge on lipoprotein production. Secretion of mutant forms of apoB36 were studied in Cos-1 cells. The values are the percent of apoB secreted following a three hour chase divided by total intracellular apoB at time zero after a one hour labelling. Values are the mean \pm SD. Experiments undertaken only twice have no SDs.

residues 1-590; and apoB16, residues 1-720) to interact with MTP. The amounts of MTP co-immunoprecipitated with each apoB polypeptide was determined by phosphorimager analysis. From these values, we subtracted the small amount of MTP co-immunoprecipitated with the control protein, apoAI. On a mole to mole basis, the interactions of apoB3.4 to apoB13 with MTP were comparable to each other and around double that between apoB16 and MTP (Figure 6(b)). The small amount of MTP-FLAG co-immunoprecipitated with the control protein apoAI was, on a mole to mole basis, 15-fold less than that immunoprecipitated with the smaller apoB constructs (Figure 6(b)). Thus, these studies assign the initial MTP binding site on apoB to the extreme amino-terminal 3.4% of apoB.

To identify the binding site on MTP for apoB, we compared the ability of haemagglutinin (HA)-tagged apoB4.5 (apoB4.5-HA) to interact with the soluble amino-terminal region of MTP (amino acid residues 22-297) and the full-length MTP protein. Anti-HA immunocomplexes prepared from cells expressing apoB4.5-HA with either the β -barrel of MTP, or with the full-length MTP, contained comparable amounts of MTP (Figure 6(c)). Control anti-apoAI immunocomplexes from cells expressing apoAI and MTP contained no MTP (Figure 6(c)). These results define the amino-terminal β -barrel of MTP between amino acid residues 22 and 297 as the region that interacts with amino acid residues 1-152 of apoB. Consistent with the mapping of the MTP-binding site on apoB to the first seven strands of its β -barrel (amino acid residues 21-154), we find that the disruption of the conserved amino-terminal apoB C159-C185 linkage, predicted to tether β -strands 8 and 9, did not impair the interaction between apoB5.8 (amino acid residues 1-252) and the amino-terminal β -barrel of MTP (Figure 5(d)).

Mutation of conserved motifs in apoB prevents secretion

Finally, we evaluated the importance of the conserved C159-C185 disulphide linkage and of the buried R531-E557-D524 salt bridge for lipoprotein assembly and secretion, by disrupting these structures in apoB36. C185A, R531H, R531A and E557A were individually created in apoB36. E560A was created as a control. The C185A mutation was also combined with C159A, R531A and R531H. ApoB36 was expressed with MTP since the secretion of apoB polypeptides longer than apoB22 requires MTP-mediated lipid transfer activity (Leiper *et al.*, 1994; Gordon *et al.*, 1994). Disruption of the disulphide linkage between C159 and C185 in apoB36 modestly decreased the production of apoB-containing lipoproteins to 58(\pm 6)% of wild-type (Figure 6(e)). The corresponding values for the R531H and R531A mutations were 39(\pm 7)% and 64(\pm 29)%, respectively. The double mutants

C185A-R531H and C185A-R531A had more profound effects, reducing apoB secretion to 13(\pm 4)% and 23(\pm 10)%, respectively. The control double mutant C159A-C185A behaved as the C185A protein (data not shown). The control mutant (E560A) and E557A did not differ from wild-type. Thus, mutation of the apoB buried salt bridge residue, R531, and of the C159-C185 cystine that has a marked impact on the secretion of apoB17 (Figure 3(b)), has a less dramatic effect on the secretion of apoB36. Similarly, the modest deleterious effect of mutating E557 in apoB17 is ameliorated in apoB36. From these results we conclude that certain disruptions of structure that prevent the secretion of the more discrete soluble forms of apoB can be overcome by the ability of the carboxyl-terminal portions of apoB to acquire a neutral lipid core.

Discussion

We have superimposed the primary sequence of the amino-terminal regions of MTP and apoB on the crystal structure of lamprey LV to derive structural information on the two key proteins required for cholesterol and triglyceride transport in vertebrates. This approach was adopted since both proteins present a formidable challenge to the crystallographer on account of their unusually large size (155 kDa and 512 kDa) and variable lipid content. While our modelling data cannot supersede the detailed atomic coordinates obtained by X-ray crystallography, it has shed important light on the overall features of the regions of MTP that interact with PDI and apoB, and provided a useful structural model as to how the lipid-binding and transfer structures of MTP might become aligned with the lipid-binding structures of newly synthesised apoB during the lipoprotein assembly process. We propose that the amino-terminal β -barrel and the central α -helical domain of the LVs are conserved in apoB and MTP, and that the conserved α -helical homodimerization interface of LV is re-utilised by MTP to form a stable heterodimer with PDI. In addition, our results provide a unifying scheme for the invertebrate origins of the major vertebrate lipid transport system.

The evidence for the overall correctness of the MTP and apoB models is compelling. Each of the cysteine residues in the apoB model forms the correct disulphide linkage (Yang *et al.*, 1990) and is appropriately placed to serve an important structural or functional role. The first cysteine, C12-C61, at the extreme amino-terminal segment of apoB, is predicted to connect two loop structures, the second of which precedes β -strand 3 of its predicted β -barrel. This region is further constrained by a disulphide linkage between C51 and C70. Disruption of this cysteine virtually abolishes the production of apoB-containing lipoproteins (Huang & Shelness, 1997). In our model, the C51-C70 cystine tethers β -strands 2 and 3, which are amongst the

longest in the β -barrel of apoB. However, since this linkage is not conserved in MTP or lamprey LV, it is questionable whether it is required for the structural integrity of apoB. Rather, a functional role is suggested. One possibility is that the C51-C70 cystine fine-tunes the binding site on apoB for MTP and that this interaction is critical for the co-translational loading of apoB with sufficient lipid to form a lipoprotein. Here we show that amino acid residues 1-152 of apoB, which are predicted to form the first seven strands of its β -barrel, interact with MTP, and that the highly conserved C159-C185 cystine, which links β -strands 8 and 9, is not required for this interaction, despite its importance for the structural integrity of the soluble portion of apoB. Accordingly, we suggest that the most probable binding site on apoB for MTP is centred on the extreme amino-terminal region of apoB and that the C51-C70 cystine is critical for maintaining the integrity of this binding site. The involvement of a disulphide linkage in orchestrating the fine structural properties of a binding site is a characteristic feature of a subfamily of periplasmic molecular chaperones which have an immunoglobulin-like topology (Zav'yalov *et al.*, 1997).

Further evidence for the reliability of our modelled structures derives from the finding that the central region of the α -helical domains of lamprey LV, MTP and apoB each contain a stabilising cystine. In crystalline lamprey LV, and predicted for MTP, there is a disulphide bridge connecting the end of helix 9 to the start of helix 10. In apoB, the helical region is predicted to be stabilised by two cystine groups, and, as is the case for lamprey LV, one is centred on helix 10. The other, formed by C358-C363, is found in the loop connecting helices 4 and 5. The fact that the corresponding region of lamprey LV is restrained by a partially buried salt bridge (R538/E390) suggests a similar structural role for the LV R538/E390 salt bridge and the apoB C358-C363 cystine.

An important feature of the apoB and MTP models is the presence of a stabilising buried salt bridge near the carboxyl-terminal end of their predicted α -helical domains. In lamprey LV, the buried salt bridge is formed between R547 and E574 and connects two segments of secondary structure, a helix and a short loop, near the carboxyl-terminal end of its large α -helical domain. In the MTP and apoB models similar structural roles are envisaged. The buried salt-bridge residues in MTP (R540-N531-E570) and apoB (R531-D524-E557) unite three segments of secondary structure, centred on the amino-terminal end of helix 14, the carboxyl terminus of helix 13 and the loop preceding helix 16. The proposition that MTP R540 and apoB R531 form the cationic arm of a buried salt bridge is also suggested by the finding that the equivalent residue is highly conserved in a wide range of VTGs, a feature commonly observed for a charged residue participating in a buried salt bridge (Schueler & Margalit, 1995). We demonstrate that the alanine substitution of MTP R540 and apoB R531 had a

major impact on the solubility of MTP and apoB17, respectively, whereas the equivalent mutation of ten other basic residues within the region of R540 of MTP did not. Very analogous results were reported for the ARC repressor protein of bacteriophage P22 (Milla *et al.*, 1994). The alanine substitution of 12 surface salt-bridge residues in this protein had little effect on protein stability, while the equivalent mutation of the glutamic acid residue at the centre of its buried salt bridge (R41-E36-R40) rendered the protein so unstable that it remained unfolded. In addition, we show that the alanine substitution of the predicted partners of MTP R540 (N531-E570) and apoB R531 (D524-E557) is deleterious, while the mutation of neighbouring acidic residues had no functional impact. The finding that the individual mutation of MTP N531 and E570, and apoB D524 and E557, was less deleterious than the mutation of MTP R540 and apoB R531 is once again analogous to the situation observed in the ARC repressor protein. In this system, the individual substitution of either of the two partners of E36 was less deleterious than the equivalent mutation of E36 itself.

Previous studies have established that many aberrantly folded proteins are retained in the ER (Gething & Sambrook, 1992). This may explain our mutagenesis studies, which show that mutation of the conserved apoB C159-C185 cystine and of the predicted R531-D524-E557 buried salt bridge is deleterious for the secretion of apoB17. The nature of the mechanism for the retention of these conformationally compromised apoBs is unknown. Proteins that are misfolded in the ER tend to associate with ER-resident proteins and form macromolecular aggregates (Bonnerot *et al.*, 1994; Le *et al.*, 1992; Melnick *et al.*, 1994; Kim *et al.*, 1992). Here we show that the interaction between MTP and the amino-terminal binding site on apoB is increased two to threefold by mutation of the conserved apoB C159-C185 cystine. These observations, and the fact that the equivalent cystine mutation in apoB36 has only a modest impact on apoB secretion, indicates that certain misfolded apoBs can be rescued from retention in the ER as their lipid binding structures receive sufficient lipid from the MTP-PDI heterodimer to incorporate a neutral lipid core. This suggests a paradigm whereby the MTP-PDI complex acts as a chaperone for nascent apoB and that the resulting lipoprotein complex proceeds along the secretory pathway, gathering lipid, until apoB attains a soluble conformation and dissociates as a secretable lipoprotein from the MTP-PDI heterodimer.

The capture and permanent binding of the VTG ancestor of MTP by the ER-resident chaperone-like protein, PDI, was an important event in the origins of apoB-containing lipoproteins. Based on the present data we propose that the PDI-binding site on MTP has emerged from structural changes to the α -helical homodimerization interface of LV. In crystalline lamprey LV, the interfacial residues form a hydrophobic plate that encompasses the

entire exposed surface of outer helices 13, 15 and 17. Here we show that the corresponding helical region (amino acid residues 520-603) interacts with PDI in a yeast two-hybrid system, whereas helices 1-8 (amino acid residues 297-442), 9-13 (amino acid residues 447-529), the predicted β -barrel (amino acid residues 22-304) and the carboxyl-terminal lipid-binding domains (amino acid residues 604-894) of MTP do not. Moreover, the alanine substitution of the solvent-exposed residues Y554, M555, K558 and I592, which are predicted to reside in a hydrophobic-enriched environment near the amino-terminal ends of helices 15 and 17 of MTP, impair PDI binding in both the yeast two-hybrid system and in a Cos-1 cell expression system. These observations and the fact that residues corresponding to MTP Y554, M555, K558 and I592 in lamprey LV (V561, A562, S565 and D600) participate in LV homodimerization lead us to the almost inevitable conclusion that the MTP-PDI heterodimerization process requires a binding site near the carboxyl-terminal end of the α -helical domain of MTP.

The defining difference between the VTGs, MTP and apoB relates to their carboxyl-terminal lipid-binding structures which associate with different types and amounts of lipid. In lamprey LV, an extensive β -sheet structure comprising some 450 residues (amino acid residues 188-190, 778-948, 991-1074 and 1358-1529) forms the bulk of the molecular surface of its lipid-binding cavity. The homologous domain in MTP is significantly truncated, indicating that it forms a smaller lipid-binding cavity. This is consistent with the much smaller ratio of lipid to protein in MTP, three compared to 38 or more in lamprey LV (Timmins *et al.*, 1992; Atzel & Wetterau, 1994). In apoB, extensive lipid-binding structures are required for the incorporation of a neutral lipid core. These have been proposed to be formed from two large amphipathic β -pleated sheet structures (amino acid residues 720-2102 and 2561-4061), alternated with two amphipathic α -helical domains (residues 2103-2560 and 4061-4338; Segrest *et al.*, 1994). In agreement with this, we find that there is sequence similarity (ranging from 28 to 33%) between amino acid residues 763-963, 988-1074 and 1404-1618 of apoB with the known lipid-binding β -pleated structure formed by amino acid residues 778-948, 991-1074 and 1358-1529 of lamprey LV.

The kinetics of incorporation of newly synthesized apoB100 into VLDL have been extensively studied in McA-RH7777 and HepG2 cells (Boren *et al.*, 1992, 1994). The results indicate that apoB100 is co-translationally loaded with lipid and that this process commences once the apoB polypeptide has reached a size of 80 kDa (apoB16, residues 1-720). The results of the present study, our recent observations (Bradbury *et al.*, 1998), and those of Hussain *et al.*, 1998, which establish that residues corresponding to the carboxyl terminus of the predicted α -helical domain of apoB also bind to MTP, suggest a

model whereby this is facilitated. The extreme amino-terminal region of newly synthesized apoB interacts with the amino terminus of MTP. The binding of the amino terminus of apoB to the MTP-PDI heterodimer forms an anchor for the interaction of amino acid residues 512-721 of the elongating apoB polypeptide to the carboxyl-terminal region of the predicted α -helical region of MTP (Bradbury *et al.*, 1998). The two sites of interaction between apoB and MTP would position the predicted lipid-binding cavity of MTP with the lipid-binding structures of apoB, and presumably initiate the co-translational transfer of lipid to apoB from MTP.

In conclusion, the structural and functional evolution of LV, apoB and MTP are herein documented. We show remarkable conservation of tertiary structure between the amino-terminal β -barrel and α -helical domains of the three proteins. Important features of the quaternary structure of the lamprey LV homodimer are retained and adapted by MTP and apoB for use in vertebrate lipoprotein assembly. These structures were evidently already established in the LVs of the nematodes where it may be presumed, as with other LVs, that they serve to deliver nutrients to the egg by receptors of the LDL-receptor family. Our phylogenetic analysis of the mammalian MTPs and of the VTGs accords well with the emergence of apoB prior to MTP and the VTGs of egg-laying vertebrates. These observations and the identification of the insect homologues of apoB indicate that the mechanism of lipid transport and clearance found in modern organisms was established in invertebrates before the development of a pressurized vascular system.

Materials and Methods

Database searches and phylogenetic analysis

Screening of the PDB, SwissProt + Spubdate + PIR and the non-redundant GenBank CDS translation databases was performed with an enhanced version of the BLAST program (Altschul *et al.*, 1997), WU-BLASTP, using the National Centre for Biotechnology Information's BLAST WWW server. The initial searchtools were the first 1000 amino acid residues of lamprey VTG and apoB. The scoring matrix was blosum 62. The most significant matches with the VTG sequence were for tobacco hornworm (*M.s*) ALP, human (*H.s*) apoB, *Drosophila melanogaster* (*D.m*) RFBP and MTP, the *P*-values being 3.4×10^{-16} , 2.2×10^{-14} , 1.6×10^{-12} and 2.7×10^{-8} , respectively. The most significant matches with the apoB sequence were for *M.s* ALP, *D.m* RFBP, *Xenopus laevis* (*X.l*) VTG, killifish (*F.h*) VTG and lamprey (*Lu*) VTG, the *P*-values being 5.2×10^{-22} , 6.2×10^{-19} , 2.8×10^{-13} , 1.4×10^{-12} and 4.6×10^{-11} , respectively. The phylogenetic tree was constructed with an alignment of the first 650 amino acid residues of 18 protein sequences: *H.s* MTP (accession number X75500); bovine (*B.t*) MTP (X78567); mouse (*M.m*) MTP; golden hamster (*M.a*) MTP (U14995); chicken (*G.g.*) VTG (X13607); *X.l* VTG (Y00354); *F.h* VTG 1 and 2 (U07055 and U70826); white

sturgeon (*A.t*) VTG (U00455); rainbow trout (*O.m*) VTG (X92804); *L.u* VTG (M88749); *D.m* RFBP (U62892); *M.s* ALP (U57651); *Caenorhabditis elegans* (*C.e*) 1 VTG; *C.e* 2 VTG (X56212); *C.e* 5 VTG (M11497 and X03044); *C.e* 6 VTG (X56213); and rhabditid nematode (*O.s*) VTG (U35449). We thank Professor L. Chan (Baylor College, of Medicine) for the *M.m* MTP sequence. The alignment was produced with the CLUSTAL version W1.6 program using default values and with minimal manual adjustment (Higgins *et al.*, 1992). The phylogenetic analysis was performed with the Seqboot, Protpars and Consense programs of the computer package PHYLIP 3.572 (Felsenstein, 1997).

Modelling

INSIGHT interactive graphics software and the DISCOVER computer program package (Biosym Technologies, San Diego CA, USA) were used. The template was the final refined X-ray crystallographic structure of lamprey LV (*R*-factor of 19% at 2.8 Å resolution; Anderson *et al.*, 1998), the coordinates of which have been deposited with the Brookhaven Protein Data Bank (accession number 1LLV). Models were developed using an alignment based on sequences from lamprey and *X laevis* LV, human MTP and apoB and *D melanogaster* RFBP. Slight manual adjustments were made to the aligned sequences to keep insertions and deletions in the loops of the lamprey LV structure. Coordinates for the structurally conserved regions were obtained directly from the crystal coordinates of lamprey LV using the Homology module of the DISCOVER program, as were the coordinates of common side-chains. Side-chains that had additional and/or different atoms were given extended conformation from the point where continuity ended. Candidate loop conformations were extracted from the Brookhaven database using a loop search procedure (Jones & Thirup, 1986). Loops with sequences as similar as possible to LV and with a good spatial fit onto the adjacent protein backbone were selected. The loop connecting helices 8 and 9 of MTP was fitted using the Protein Database fragment library in the O program (Jones *et al.*, 1991). It was the 20th best fit and had an overall conformation most similar to the corresponding loop in LV. Steric clashes between several large side-chains were removed manually and replaced with rotamers using a rotamer database inside the O program (Jones *et al.*, 1991). Steepest descent energy minimization was utilized to reposition all atoms with a van der Waals overlap greater than 0.5 Å. Bond length and bond and torsion angles were regularized in the O program until convergence was reached. Emerging models underwent energy minimization using X-PLOR (Brunger, 1992). Disulphide bonds were restrained by disulphide bond parameters. The energy gradient was driven to convergence by several hundred cycles of conjugate gradient energy minimization, followed by minor model rebuilding. The quality of the coordinates were continually assessed using PROCHECK (Laskowski *et al.*, 1993) and X-PLOR (Brunger, 1992). The quality of non-covalent interactions was assessed with ERRAT (Colovos & Yeates, 1993). Lysine was introduced into the final MTP model using the O program. The predicted surface area of solvent-accessibility was calculated using X-PLOR. Three-dimensional solid-model representations of apoB and MTP were drawn using the program SETOR (Evans, 1993).

Identification of MTP R540H

A description of the patient and the sequencing methodology have been published (Willemin *et al.*, 1987; Narcisi *et al.*, 1995).

Construction of expression vectors and mutagenesis

Details of oligonucleotides are available on request (C.C.S.). PCR and appropriate restriction sites were used to manipulate the MTP, apoB and PDI sequences. Epitope tags were fused in-frame to the carboxyl termini of cDNAs and juxtaposed to a terminator codon. The sequences of the FLAG and HIS epitopes were Asp-Tyr-Lys-Asp₄-Lys and His₆, respectively. The vectors for the baculovirus work were pVL1392 and 1393 (Invitrogen, Netherlands). All constructs were sequenced before use. The mutagenesis of MTP was facilitated by the introduction of a *Bgl*III recognition site (nucleotides 1933-1938) into MTP cDNA (Shoulders *et al.*, 1993; Leiper *et al.*, 1994); this did not alter the encoded sequence. Site-directed mutagenesis was by a two-step PCR-based strategy.

Expression of MTP in Cos-1 cells

Cos-1 cells (2×10^7) were transfected with 50 µg of MTP-FLAG and 25 µg of β-galactosidase control plasmid as described (Leiper *et al.*, 1994; Narcisi *et al.*, 1995). Cells were harvested 36 hours post-transfection, lysed on ice by probe-sonication, and a soluble fraction obtained by centrifugation at 100,000 *g* for 60 minutes at 4°C as described (Rehberg *et al.*, 1996). Cell pellets were washed and recovered by probe-sonication. MTP was detected with either mouse anti-FLAG M2 antibody (Kodak IBI Anachem) or rabbit anti-human MTP-PDI antiserum, diluted to 1:333 and 1:500, respectively. Anti-serum to the human MTP-PDI complex was obtained from rabbits immunized with recombinant MTP complex. Triglyceride transfer-activity assays were undertaken as described (Narcisi *et al.*, 1995).

Yeast two hybrid system

The vectors pSB202, pJG4-5 and the LacZ reporter gene plasmid, pSH18-34, were kind gifts from Professor R. Brent (Harvard Medical School, Massachusetts, USA; Gyuris *et al.*, 1993; Zervos *et al.*, 1993). The yeast strain was EGY48. MTP was fused to the amino terminus of Lex A and assayed for interaction with PDI fused to the B42 transcription activation domain. The MTP constructs represented the amino-terminal β-sheet region (residues 22-304), the entire α-helical domain (298-603), the carboxyl-terminal domain (604-894) and predicted helices 1-8 (297-442), 9-13 (447-529), 9-17 (447-603) and 13-17 (517-603), respectively. PDI constructs were created with a clone containing the human full-length PDI cDNA sequence, a kind gift from Professor K. I. Kivirikko (Collagen Research Unit, University of Oulu, Finland). The PDI constructs represented domains ae (amino acid residues 18-173), aeb (amino acid residues 18-273) and the full-length protein (amino acid residues 18-508). Transformation and β-galactosidase activity assays were undertaken as described (Reynolds & Lundblad, 1992). Fusion proteins were detected by immunoblotting. The LexA antibody was purchased from Clontech (Basingstoke, UK).

Baculovirus expression and microsomal preparations

Sf9 cells were maintained as monolayers in Grace's medium (Gibco-BRL, Life Technologies, Paisley, UK), supplemented with 10% (v/v) insect-qualified foetal calf serum (Gibco-BRL). Transfections were with liposomes, linearized BacPAK 6 viral DNA (Clontech) and the appropriate baculovirus transfer vectors (Invitrogen). Recombinant viruses were plaque-purified and high-titre stocks generated. We thank Dr David Booth (Imperial College School of Medicine, London) for the recombinant apoAI virus. Cells were infected at a multiplicity of 2.5 and harvested 42-46 hours post-infection. Cells for labelling were washed and re-suspended in 7 ml of methionine-free Grace's medium and gently agitated at 27°C for 45 minutes. Labelling commenced with the addition of 0.43 mCi of L-[³⁵S]methionine (Pro-Mix, Amersham International PLC, Buckinghamshire, UK) and continued for 75 minutes. Analysis of expression was undertaken on microsomal fractions, which were at all stages maintained at 4°C. To obtain microsomes, cells were washed in phosphate-buffered saline (PBS), homogenized in 0.25 M sucrose containing 20 mM imidazole (pH 7.4) and protease inhibitors, layered onto a discontinuous gradient of 1.8 M sucrose in 20 mM imidazole and 0.5 M sucrose in 20 mM imidazole, and centrifuged at 100,000 g for 60 minutes. The pellicle of microsomes at the 0.5-1.8 M sucrose interface was resuspended in 10 mM Tris (pH 7.4), 150 mM NaCl, with the specified detergent. The radioactivity in expressed proteins was quantified by phosphorimager analysis (Molecular Dynamics, Buckinghamshire, UK).

Affinity purification of PDI(HIS)

Microsomes were solubilized with 0.2% (w/v) deoxycholate in 10 mM Tris (pH 7.4), 150 mM NaCl, at a protein concentration of 300 µg/ml and cleared of insoluble material by centrifugation at 100,000 g for one hour as described (Rehberg *et al.*, 1996). PDI-HIS was affinity purified with saturating quantities of anti-HIS resin (TALON) as recommended by the manufacturer (Clontech).

Immunoprecipitations

ApoB, apoAI, apoB-HA and MTP-FLAG were immunoprecipitated with saturating quantities of anti-apoB (Boehringer, Roche Diagnostics Ltd, E. Sussex, UK), anti-apoAI (Genzyme Diagnostics, Kent, UK) and anti-HA (Cambridge Bioscience, UK) antibodies, and anti-FLAG M2 affinity gel (Kodak IBI), respectively. Immobilized proteins were washed exhaustively with immunoprecipitation buffer (1% (v/v) Triton X-100 in 10 mM Tris (pH 7.4), containing 150 mM NaCl, 2 mM EDTA and protease inhibitors), recovered by boiling in SDS sample buffer and separated by SDS-PAGE.

Expression of apoB in Cos-1 cells

The construction of B17 and B36 has been reported (White *et al.*, 1992), as has the transfection and L-[³⁵S]methionine labelling of cells and the immunoprecipitation of apoB (Leiper *et al.*, 1994). For optimal levels of secretion, apoB17 was chased for two hours and apoB36 for three hours.

Protein Data Bank Accession Number

The atomic coordinates for and the apoB and MTP models have been deposited with the Protein Data Bank, Brookhaven National Laboratory, USA. The accession number for lamprey LV is 1LLV.

Acknowledgements

We gratefully acknowledge the financial support from the British Medical Research Council and the British Heart Foundation (Grant numbers PG/95186, PG/96101 and PG/97011). J.S. also gratefully thanks the Bristol-Myers Squibb Corporation for a cardiovascular research award. We thank Professor Robert Brasseur, Drs Naveenan Navaratnam and Andrew F. Dean for helpful discussion, Teresa Narcisi, Tamsin Grantham and Dianne Sullivan for assistance at the early stages of the project, and Mrs Glennis McDonald for help in preparing the manuscript. We are also grateful to Professor Dimitris Cournaros and Drs Isabel Beucler, Veronique Clavey and Daniel Pinsebert for clinical assistance. Modelling activities were supported by a US-NIH grant (GH 13925) and the Minnesota Supercomputer Institute (University of Minnesota).

References

- Altschul, S. F., Madden, T. L., Schaffer, A. A., Zhang, J., Zhang, Z., Miller, W. & Lipman, D. J. (1997). Gapped BLAST and PSI-BLAST - a new generation of protein database search programs. *Nucl. Acids Res.* **25**, 3389-3402.
- Anderson, T. A., Levitt, D. G. & Banaszak, L. J. (1998). Crystal structure of lamprey lipovitellin, a member of a novel class of lipid-carrying proteins. *Structure*, **6**, 895-909.
- Atzel, A. & Wetterau, J. R. (1994). Identification of two classes of lipid molecule binding sites on the microsomal triglyceride transfer protein. *Biochemistry*, **33**, 15382-15388.
- Baker, M. E. (1988). Is vitellogenin an ancestor of apolipoprotein B-100, of human low-density lipoprotein and human lipoprotein lipase? *Biochem. J.* **255**, 1057-1060.
- Bonnerot, C., Marks, M. S., Cosson, P., Robertson, E. J., Bikoff, E. K., Germain, R. N. & Bonifacino, J. S. (1994). Association with BiP and aggregation of class II MHC molecules synthesized in the absence of invariant chain. *EMBO J.* **13**, 934-944.
- Boren, J., Graham, L., Wettsten, M., Scott, J., White, A. & Olofsson, S.-O. (1992). The assembly and secretion of apoB 100-containing lipoproteins in HepG2 cells. *J. Biol. Chem.* **267**, 9858-9867.
- Boren, J., Rustaeus, S. & Olofsson, S.-O. (1994). Studies on the assembly of apolipoprotein B-100- and B-48-containing very low density lipoproteins in McA-RH7777 cells. *J. Biol. Chem.* **269**, 25879-25888.
- Bradbury, P., Mann, C. J., Köchl, S., Anderson, T. A., Chester, S. A., Hancock, J. M., Ritchie, P. J., Amey, J., Levitt, D. G., Banaszak, L. J., Scott, J. & Shoulders, C. C. (1998). A common binding site on the microsomal triglyceride transfer protein for apolipoprotein B and protein disulphide isomerase, *J. Biol. Chem.* In the press.

- Brown, M. S., Herz, J. & Goldstein, J. L. (1997). Calcium cages, acid baths and recycling receptors. *Nature*, **388**, 629-630.
- Brunger, A. T. (1992). *X-PLOR (Version 3.1). A System for X-ray Crystallography and NMR*, Yale University Press, New Haven, CT.
- Bujo, H., Yamamoto, T., Hayashi, K., Hermann, M., Nimpf, J. & Schneider, W. J. (1995). Mutant oocytic low density lipoprotein receptor gene family member causes atherosclerosis and female sterility. *Proc. Natl Acad. Sci. USA*, **92**, 9905-9909.
- Byrne, B. M., Gruber, M. & Ab, G. (1989). The evolution of egg yolk proteins. *Prog. Biophys. Mol. Biol.* **53**, 33-69.
- Chatterton, J. E., Phillips, M. L., Curtiss, L. K., Milne, R., Fruchart, J. C. & Schumaker, V. N. (1995). Immunoelectron microscopy of low density lipoproteins yields a ribbon and bow model for the conformation of apolipoprotein B on the lipoprotein surface. *J. Lipid Res.* **36**, 2027-2037.
- Clackson, T. & Wells, J. A. (1995). A hot spot of binding energy in a hormone-receptor interface. *Science*, **267**, 383-386.
- Colovos, C. & Yeates, T. O. (1993). Verification of protein structures: patterns of nonbonded atomic interactions. *Protein Sci.* **2**, 1511-1519.
- Evans, S. V. (1993). SETOR: hardware-lighted three-dimensional solid model representations of macromolecules. *J. Mol. Graph.* **11**, 134-138.
- Felsenstein, J. (1997). *Phylogeny Inference Package, Version 3.5c*. Distributed by the author, Department of Genetics, University of Washington, Seattle, USA.
- Gething, M.-J. & Sainbrook, S. (1992). Protein folding in the cell. *Nature*, **355**, 33-45.
- Golemis, E. A. & Brent, R. (1992). Fused protein domains inhibit DNA binding by LexA. *Mol. Cell Biol.* **12**, 3006-3014.
- Gordon, D. A., Jamil, H., Sharp, D., Mullaney, D., Yao, Z., Gregg, R. E. & Wetterau, J. (1994). Secretion of apolipoprotein B-containing lipoproteins from HeLa cells is dependent on expression of the microsomal triglyceride transfer protein and is regulated by lipid availability. *Proc. Natl Acad. Sci. USA*, **91**, 7628-7632.
- Gretch, D. G., Sturley, S. L., Wang, L., Lipton, B. A., Dunning, A., Grunwald, K. A. A., Wetterau, J. R., Yao, Z., Talmud, P. & Attie, A. D. (1996). The amino terminus of apolipoprotein B is necessary but not sufficient for microsomal triglyceride transfer protein responsiveness. *J. Biol. Chem.* **271**, 8682-8691.
- Gyuris, J., Golemis, E., Chertkov, H. & Brent, R. (1993). Cdi1, a human G1 and S phase protein phosphatase that associates with Cdk2. *Cell*, **75**, 791-803.
- Higgins, D. G., Bleasby, A. J. & Fuchs, R. (1992). CLUSTAL V: improved software for multiple sequence alignment. *Comput. Applic. Biosci.* **8**, 189-191.
- Huang, X. F. & Shelness, G. S. (1997). Identification of cysteine pairs within the amino-terminal 5% of apolipoprotein B essential for hepatic lipoprotein assembly and secretion. *J. Biol. Chem.* **272**, 31872-31876.
- Hussain, M. M., Bakillah, A., Nayak, N. & Shelness, G. S. (1998). Amino acids 430-570 in apolipoprotein B are critical for its binding to microsomal triglyceride transfer protein. *J. Biol. Chem.* **273**, 25612-25615.
- Janin, J., Miller, S. & Chothia, C. (1988). Surface, subunit interfaces and interior of oligomeric proteins. *J. Mol. Biol.* **204**, 155-164.
- Jones, T. A. & Thirup, S. (1986). Using known substructures in protein model building and crystallography. *EMBO J.* **5**, 819-822.
- Jones, T. A., Zou, J. Y., Cowan, S. W. & Kjeldgaard, M. (1991). Improved methods for binding protein models in electron density maps and the location of errors in these models. *Acta Crystallog. sect. A*, **47**, 110-119.
- Kane, J. P. & Havel, R. J. (1989). Disorders of the biogenesis and secretion of lipoproteins containing the B apolipoproteins. In *The Metabolic Basis of Inherited Disease* (Scriver, C. R., Beaudet, A. L., Sly, W. S. & Valle, D., eds), pp. 1139-1164, McGraw-Hill, New York.
- Kim, P. S., Bole, D. & Arvan, P. (1992). Transient aggregation of nascent thyroglobulin in the endoplasmic reticulum: relationship to the molecular chaperone, BiP. *J. Cell Biol.* **118**, 541-549.
- Knott, T. J., Pease, R. J., Powell, L. M., Wallis, S. C., Rall, S. C., Jr, Innerarity, T. L., Blackhart, B., Taylor, W. H., Marcel, Y., Milne, R., Johnson, D., Fuller, M., Lusi, A. J., McCarthy, B. J., Mahley, R. W., Levy-Wilson, B. & Scott, J. (1986). Complete protein sequence and identification of structural domains of human apolipoprotein B. *Nature*, **323**, 734-738.
- Kutty, R. K., Kutty, G., Kambadur, R., Duncan, T., Koonin, E. V., Rodriguez, I. R., Odenwald, W. F. & Wiggert, B. (1996). Molecular characterization and developmental expression of a retinoid- and fatty acid-binding glycoprotein from *Drosophila*. A putative lipophorin. *J. Biol. Chem.* **271**, 20641-20649.
- Lamberg, A., Jauhainen, J., Metso, J., Ehnholm, C., Shoulders, C., Scott, J., Pihlajaniemi, T. & Kivirikko, K. I. (1996). The role of protein disulphide isomerase in the microsomal triacylglycerol transfer protein does not reside in its isomerase activity. *Biochem. J.* **315**, 533-536.
- Laskowski, R. A., MacArthur, M. W., Moss, D. S. & Thornton, J. M. (1993). PROCHECK: a program to check the stereochemical quality of a protein structure. *J. Appl. Crystallog.* **26**, 283-291.
- Law, A. & Scott, J. (1990). A cross-species comparison of the apolipoprotein B domain that binds to the LDL receptor. *J. Lipid Res.* **31**, 1109-1120.
- Le, A., Ferrell, G. A., Dishon, D. S., Le, Q. Q. & Sifers, R. N. (1992). Soluble aggregates of the human PiZ alpha 1-antitrypsin variant are degraded within the endoplasmic reticulum by a mechanism sensitive to inhibitors of protein synthesis. *J. Biol. Chem.* **267**, 1072-1080.
- Leiper, J. M., Bayliss, J. D., Pease, R. J., Brett, D. J., Scott, J. & Shoulders, C. C. (1994). Microsomal triglyceride transfer protein, the abetalipoproteinemia gene product, mediates the secretion of apolipoprotein B-containing lipoproteins from heterologous cells. *J. Biol. Chem.* **269**, 21951-21954.
- Linton, M. F. & Farese, R. V. J. (1997). Familial hypobetalipoproteinemia. *J. Lipid Res.* **34**, 521-541.
- Melnick, J., Dul, J. L. & Argon, Y. (1994). Sequential interaction of the chaperones BiP and GRP94 with immunoglobulin chains in the endoplasmic reticulum. *Nature*, **370**, 373-375.
- Milla, M. E., Brown, B. M. & Sauer, R. T. (1994). Protein stability effects of a complete set of alanine substitutions in Arc repressor. *Struct. Biol.* **1**, 518-523.
- Narcisi, T. M. E., Shoulders, C. C., Chester, S. A., Read, J., Brett, D. J., Harrison, G. B., Grantham, T. T., Fox, M. F., Povey, S., de Bruin, T. W. A., Erkelens, D. W., Muller, D. P. R., Lloyd, J. K. & Scott, J. (1995).

- Mutations of the microsomal triglyceride-transfer-protein gene in abetalipoproteinemia. *Am. J. Hum. Genet.* **57**, 1298-1310.
- Nichols, J. C. & Matthews, K. S. (1997). Combinational mutations of *lac* repressor. Stability of monomer-monomer interface is increased by apolar substitution at position 84. *J. Biol. Chem.* **272**, 18550-18557.
- O'Neill, K. T. & DeGrado, W. F. (1990). A thermodynamic scale for the helix-forming tendencies of the commonly occurring amino acids. *Science*, **250**, 646-651.
- Patel, S. & Grundy, S. (1996). Interactions between microsomal triglyceride transfer protein and apolipoprotein B within the endoplasmic reticulum in a heterologous expression system. *J. Biol. Chem.* **271**, 18686-18694.
- Poortinga, G., Watanabe, M. & Parkhurst, S. M. (1998). *Drosophila* CtBP: a Hairy-interacting protein required for embryonic segmentation and hairy-mediated transcriptional repression. *EMBO J.* **17**, 2067-2078.
- Raag, R., Appelt, K., Xuong, N.-X. & Banaszak, L. (1988). Structure of the lamprey yolk lipid-protein complex lipovitellin-phosvitin at 2.8 Å resolution. *J. Mol. Biol.* **200**, 553-569.
- Rehberg, E. F., Samson-Bouma, M.-E., Kienzle, B., Blinderman, L., Jamil, H., Wetterau, J. R., Aggerbeck, L. P. & Gordon, D. A. (1996). A novel abetalipoproteinemia genotype. *J. Biol. Chem.* **271**, 29945-29952.
- Reynolds, A. & Lundblad, V. (1992). Yeast vectors and expression assays. In *Short Protocols in Molecular Biology* (Ausubel, F. M., Brent, R. & Kingston, R. E., et al., eds), Greene Publishing Associates and John Wiley, New York.
- Ricci, B., Sharp, D., O'Rourke, E., Kienzle, B., Blinderman, L., Gordon, D., Smith-Monroy, C., Robinson, G., Gregg, R. E., Rader, D. J. & Wetterau, J. R. (1995). A 30-amino acid truncation of the microsomal triglyceride transfer protein large subunit disrupts its interaction with protein disulfide-isomerase and causes abetalipoproteinemia. *J. Biol. Chem.* **270**, 14281-14285.
- Sattler, M., Liang, H., Nettlesheim, D., Meadows, R. P., Harlan, J. E., Eberstadt, M., Yoon, H. S., Shuker, S. B., Chang, B. S., Minn, A. J., Thompson, C. B. & Fesik, S. W. (1997). Structure of Bcl-xL-Bak peptide complex: recognition between regulators of apoptosis. *Science*, **275**, 963-966.
- Schueler, O. & Margalit, H. (1995). Conservation of salt bridges in protein families. *J. Mol. Biol.* **248**, 125-135.
- Schwartz, R. M. & Dayhoff, M. O. (1979). Matrices for detecting distant relationships. In *Atlas of Protein Sequence and Structure* (Dayhoff, M. O., ed.), vol. 5 (suppl.3), chapt. 23, pp. 353-358, Washington DC National Biomedical Research Foundation, Washington DC.
- Segrest, J. P., Jones, M. K., Mishra, V. K., Anantharamaiah, G. M. & Garber, D. W. (1994). ApoB-100 has a pentameric structure composed of three amphipathic α -helical domains alternating with two amphipathic β -strand domains. *Arterioscler. Thromb.* **14**, 1674-1685.
- Sharp, D., Blinderman, L., Combs, K. A., Kienzle, B., Ricci, B., Wager-Smith, K., Gil, C. M., Turck, C. W., Bourn, M. E., Rader, D. J., Aggerbeck, L. P., Gregg, R. E., Gordon, D. A. & Wetterau, J. R. (1993). Cloning and gene defects in microsomal triglyceride transfer protein associated with abetalipoproteinemia. *Nature*, **365**, 65-69.
- Shelness, G. S. & Thornburg, J. T. (1996). Role of intramolecular disulfide bond formation in the assembly and secretion of apolipoprotein B-100-containing lipoproteins. *J. Lipid Res.* **37**, 408-419.
- Shoulders, C. C., Brett, D. J., Bayliss, J. D., Narcisi, T. M., Jarmuz, A., Grantham, T. T., Leoni, P. R. D., Bhattacharya, S., Pease, R. J., Cullen, P. M., Levi, S., Byfield, P. G. H., Purkiss, P. & Scott, J. (1993). Abetalipoproteinemia is caused by defects of the gene encoding the 97 kDa subunit of a microsomal triglyceride transfer protein. *Hum. Mol. Genet.* **2**, 2109-2116.
- Shoulders, C. C., Narcisi, T. M. E., Read, J., Chester, S. A., Brett, D. J., Scott, J., Anderson, T. A., Levitt, D. G. & Banaszak, L. J. (1994). The abetalipoproteinemia gene is a member of the vitellogenin family and encodes an α -helical domain. *Nature Struct. Biol.* **1**, 285-286.
- Timmins, P. A., Poliks, B. & Banaszek, L. (1992). The location of bound lipid in the lipovitellin complex. *Science*, **257**, 652-655.
- Tissot, A. C., Vuilleumier, S. & Fersht, A. R. (1996). Importance of two buried salt bridges in the stability and folding pathway of barnase. *Biochemistry*, **35**, 6786-6794.
- Veijola, J., Pihlajaniemi, T. & Kivirikko, K. I. (1996). Co-expression of the alpha subunit of human prolyl 4-hydroxylase with BiP polypeptide in insect cells leads to the formation of soluble and insoluble complexes. Soluble alpha-subunit-BiP complexes have no prolyl 4-hydroxylase activity. *Biochem. J.* **315**, 613-618.
- Waldburger, C. D., Schildbach, J. F. & Sauer, R. T. (1995). Are buried salt bridges important for protein stability and conformational specificity? *Nature Struct. Biol.* **2**, 122-128.
- Wang, J., Smerdon, S. J., Jager, J., Kohlstaedt, L. A., Rice, P. A., Friedman, J. M. & Steitz, T. A. (1994). Structural basis of asymmetry in the human immunodeficiency virus type 1 reverse transcriptase heterodimer. *Proc. Natl Acad. Sci. USA*, **91**, 7242-7246.
- Welty, F. K., Seman, L. & Yen, F. T. (1995). Purification of the apolipoprotein B-67-containing low density lipoprotein particle and its affinity for the low density lipoprotein receptor. *J. Lipid Res.* **36**, 2622-2629.
- Wetterau, J. R., Combs, K. A., McLean, L. R., Spinner, S. N. & Aggerbeck, L.-P. (1991). Protein disulfide isomerase appears necessary to maintain the catalytically active structure of the microsomal triglyceride transfer protein. *Biochemistry*, **30**, 9728-9735.
- White, A. L., Graham, D. L., LeGros, J., Pease, R. J. & Scott, J. (1992). Oleate-mediated stimulation of apolipoprotein B secretion from rat hepatoma cells. *J. Biol. Chem.* **267**, 15657-15664.
- Willemin, B., Coumaros, D., Zerbe, S., Weill-Bousson, M., Annonier, P., Hirsch, E., Aby, M. A., Schmutz, G. & Bockel, R. (1987). L'abetalipoproteinemie. A propos de deux cas. *Gastroenterol. Clin. Biol.* **11**, 704-708.
- Wu, X., Zhou, M., Huang, L.-S., Wetterau, J. & Ginsberg, H. N. (1996). Demonstration of a physical interaction between microsomal triglyceride transfer protein and apolipoprotein B during the assembly of apoB-containing lipoproteins. *J. Biol. Chem.* **271**, 10277-10281.
- Yang, C.-Y., Chen, S.-H., Gianturco, S. H., Bradley, W. A., Sparrow, J. T., Tanimura, M., Li, W.-H.,

- Sparrow, D. A., DeLoof, H., Rosseneu, M., Lee, F.-S., Gu, Z.-W., Gotto, A. M., Jr & Chan, L. (1986). Sequence, structure, receptor-binding domains and internal repeats of human apolipoprotein B-100. *Nature*, **323**, 738-742.
- Yang, C.-Y., Kim, T. W., Weng, S.-A., Lee, B., Yang, M. & Gotto, A. M. J. (1990). Isolation and characterization of sulfhydryl and disulfide peptides of human apolipoprotein B-100. *Proc. Natl. Acad. Sci. USA*, **87**, 5523-5527.
- Zav'yalov, V. P., Chernovskaya, T. V., Chapman, D. A. G., Karlyshev, A. N., MacIntyre, S., Zavialov, A. N., Vasiliev, A. M., Denesyuk, A. I., Zav'yalova, G. A., Dudich, I. V., Korpela, T. & Abramov, V. M. (1997). Influence of the conserved disulphide bond, exposed to the putative binding pocket, on the structure and function of the immunoglobulin-like molecular chaperone Caf1 M of *Yersinia pestis*. *Biochem. J.* **324**, 571-578.
- Zervos, A. S., Gyuris, J. & Brent, R. (1993). Mxi1, a protein that specifically interacts with Max to bind Myc-Max recognition sites. *Cell*, **72**, 223-232.

Edited by A. R. Fersht

(Received 11 June 1998; received in revised form 30 September 1998; accepted 7 October 1998)